Effects of the surroundings and conformerisation of n-dodecane molecules on evaporation/condensation processes

Vladimir M. Gun'ko, Rasoul Nasiri, and Sergei S. Sazhin

Citation: The Journal of Chemical Physics **142**, 034502 (2015); doi: 10.1063/1.4905496
View online: http://dx.doi.org/10.1063/1.4905496
View Table of Contents: http://scitation.aip.org/content/aip/journal/jcp/142/3?ver=pdfcov
Published by the AIP Publishing

Effects of the surroundings and conformerisation of *n*-dodecane molecules on evaporation/condensation processes

Vladimir M. Gun'ko,[1,2] Rasoul Nasiri,[2] and Sergei S. Sazhin[2,a)]
[1]*Chuiko Institute of Surface Chemistry, 17 General Naumov Street, Kiev 03164 Ukraine*
[2]*Sir Harry Ricardo Laboratories, School of Computing, Engineering and Mathematics, University of Brighton, Cockcroft Building, Lewes Road, Brighton BN2 4GJ, United Kingdom*

(Received 2 October 2014; accepted 22 December 2014; published online 16 January 2015)

The evaporation/condensation coefficient (β) and the evaporation rate (γ) for *n*-dodecane *vs*. temperature, gas pressure, gas and liquid density, and solvation effects at a droplet surface are analysed using quantum chemical density functional theory calculations of several ensembles of conformers of *n*-dodecane molecules in the gas phase (hybrid functional ωB97X-D with the cc-pVTZ and cc-pVDZ basis sets) and in liquid phase (solvation method: SMD/ωB97X-D). It is shown that β depends more strongly on a number of neighbouring molecules interacting with an evaporating molecule at a droplet surface (this number is estimated through changes in the surface Gibbs free energy of solvation) than on pressure in the gas phase or conformerisation and cross-conformerisation of molecules in both phases. Thus, temperature and the surrounding effects at droplet surfaces are the dominant factors affecting the values of β for *n*-dodecane molecules. These values are shown to be similar (at reduced temperatures $T/T_c < 0.8$) or slightly larger (at $T/T_c > 0.8$) than the values of β calculated by the molecular dynamics force fields (MD FF) methods. This endorses the reliability of the previously developed classical approach to estimation of β by the MD FF methods, except at temperatures close to the critical temperature. © *2015 AIP Publishing LLC.* [http://dx.doi.org/10.1063/1.4905496]

I. INTRODUCTION

Processes of the evaporation of liquids and condensation of vapours play important roles in nature, agriculture, industry, and medicine.[1–6] These processes have various features in huge (e.g., oceans, seas, lakes, rivers, and soils) and relatively small (sprays, diesel engines, and droplets sessile at a flat surface or located in porous media) systems.[4–39] The evaporation/condensation processes depend strongly on ambient conditions (temperature, pressure, free or restricted volumes of liquid and gas, droplet sizes, gas flow rate, and level of turbulence) and types of evaporating/condensing compounds (sizes, structure, polarity of molecules, mixture composition of liquids, and presence and type of solutes).[2–15] The type of compound determines the characteristics of intermolecular interactions in liquids affecting the rates of evaporation and condensation depending on a number of parameters, including temperature, and total and partial gas (vapour) pressures.[2,3,5–15] Our analysis is focused on *n*-alkane droplets with predominant van-der-Waals (vdW) intermolecular interactions. The approach developed in this paper, however, is relatively general and can be applied to both small and large systems with nonpolar or polar compounds since it is focused mainly on the changes in the Gibbs free energy occurring due to transfer of a molecule from a liquid surface to the gas phase during evaporation and vice versa during condensation at various temperatures and pressures.

The evaporation and condensation of droplets have been studied using both experimental methods and theoretical modelling based on hydrodynamic and kinetic approaches.[5–15] Two parameters, the evaporation/condensation coefficient (β) and the evaporation rate (γ), have been used to describe these processes. The evaporation rate, γ, was considered in a number of papers based on quantum chemical (QC) methods.[38–41] It was studied for *n*-alkane molecules in the C_8-C_{27} range for molecular clusters and nanodroplets.[40,41] The analysis was based on the QC solvation method (SMD) and the kinetic gas theory, assuming that the system is in a state of thermodynamic equilibrium, i.e., the evaporation and condensation rates are equal. The kinetic gas theory was applied to estimate the collision rate of molecules/clusters/nanodroplets in the gas phase. An increase in the molecular size of evaporating alkanes resulted in a strong decrease in the values of γ.

The evaporation/condensation coefficient, β, is particularly important for kinetic modelling, where it is used for formulation of the kinetic boundary conditions at the surface of the droplet.[6,8] There are several theoretical methods and techniques used to estimate the values of β *vs*. temperature, total and partial pressures, and liquid/gas/vapour composition. In the molecular dynamics (MD) approach,[6,8,35–37] interactions between individual molecules are described by the non-reactive or reactive force fields (FF) or quantum chemical methods. *Ab initio*, density functional theory (DFT), and semiempirical QC methods are used alongside MD, trajectory, dynamic reaction coordinate, and other techniques.[38–41] It was shown that the QC *ab initio* and DFT methods with appropriate basis sets lead to more accurate modelling of the evaporation and condensation processes than semiempirical or MD FF methods. However, QC *ab initio* and DFT methods require much longer computation time for much smaller

a)E-mail address: S.Sazhin@brighton.ac.uk

droplets (clusters or nanodroplets) than MD FF. These two approaches are essentially complementary and the comparison between them can be used to justify the range of applicability of classical MD FF.

The intermolecular bonds in droplets with nonpolar or weakly polar organics (e.g., normal, iso- and cycloalkanes, and aromatics) are of the vdW type[42] characterised by relatively weak short-range forces (permanent dipole-permanent dipole, permanent dipole-induced dipole, and transitory dipole-transitory dipole interactions) controlling the behaviour of Lennard-Jones (LJ) fluids.[43,44] The vdW type of intermolecular interactions allow one to simplify the modelling using the molecular mechanics (MM) and MD methods with various vdW and LJ FF.[6,8,13–15] The models were applied to both individual liquids and complex mixtures including a number of compounds which can be evaporated under various conditions.[43–51] The reliability and the accuracy of MD FF approaches to modelling the temperature/pressure behaviour of liquid droplets and determination of the functions $\beta(T)$ and $\gamma(T)$ under various conditions, however, still need to be investigated. The present work is focused on the analysis of β as a function of temperature, pressure, gas and liquid density, and surface surrounding effects, affecting the interaction of evaporating molecules with neighbouring molecules. The analysis is based on the transition state theory (TST) and quantum chemical DFT methods applied to several ensembles of conformers of *n*-dodecane molecules. In contrast to the previous studies,[6,8] in this paper, the TST is based on a more accurate QC DFT approach taking into account the conformerisation of *n*-dodecane molecules. As in the previous studies (e.g., Ref. 41), *n*-dodecane is considered as a representative of *n*-alkanes in diesel fuel. The results are compared with the values of β previously computed using the MD FF methods.[6,8,13–15,36,37,52]

II. COMPUTATION METHODS

QC calculations were carried out using the DFT method with a hybrid functional ωB97X-D [53–55] (labelled as wB97XD in Gaussian 09) and two (cc-pVTZ (larger) and cc-pVDZ (smaller)) basis sets with the Gaussian 09 program suite.[53] The geometry of *n*-dodecane conformers was optimised using ωB97X-D/cc-pVTZ. All calculations were performed taking into account zero-point and thermal (calculating vibrational spectra) corrections to the Gibbs free energy of each conformer of *n*-dodecane. The solvation effects for *n*-dodecane conformers in *n*-dodecane medium were analysed based on the application of the SMD[56] implemented in Gaussian 09. This allowed us to compute the Gibbs free energy of solvation, $\Delta G_s = G_l - G_g$, where G_l and G_g are the Gibbs free energies of a molecule in the liquid and gas media, respectively.

Functional ωB97X-D, used in our analysis, introduces empirical damped atom-pairwise dispersion terms into the functional containing range-separated Hartree-Fock exchange for improved description of the vdW interactions.[53–57] Therefore, this functional was selected to obtain more adequate results for *n*-dodecane conformers in the gas and liquid (SMD) phases than those obtained previously using functional B3LYP.[40,41] To analyse the basis set size effects, the calculations were carried out using cc-pVTZ and cc-pVDZ, providing 724 and 298 basis functions for an *n*-dodecane molecule, respectively.

A batch of QC DFT calculations was carried out at various temperatures. Also, the temperature effects were estimated using QC results at $T_0 = 298.15$ K and certain temperature-dependent corrections for $\Delta G_{l\to g}(T) = G_g(T) - G_l(T)$ and $\Delta G_{g\to l}(T)$ (see supplementary material[58]).

For visualisation of the fields around molecules, the TorchLite (version 10.3, 2014) program was used.[59,60] Although all interactions at a molecular level are electrostatic in origin, the whole electrostatic field surrounding the molecule can be split into four types of interactions or fields, which correspond to (i) predominantly hydrophobic interactions, (ii) vdW attraction forces, and electrostatic fields dominated by (iii) electropositive or (iv) electronegative atoms or ions. In the field visualisation approach, each atom or group of atoms is considered as a "field point" of one of these four types; all field points give continuous fields.[59,60] For *n*-alkanes, the first two fields are the dominant. Visualisation of molecular structures was also performed with the help of the ChemCraft (version 1.7/382) program.[61]

Previous QC MD and dynamic reaction coordinate calculations showed[40,41] that linear, flexible, and relatively long (~1.6 nm) *n*-dodecane molecules can change their conformation in both liquid and gas phases, and these dynamic changes increase and become faster at higher temperatures. Changes in the conformer structures of *n*-alkanes can easily occur, especially at high temperatures, due to relatively low barriers to the rotations of CH_2 groups around C–C bonds.[43,44] This suggests that the effects of both the conformerisation and cross-conformerisation (changes in conformer state during transfer into another phase) of *n*-dodecane molecules (CDM) should be considered during calculations of β and γ (see supplementary material[58]).

Several approaches to the definition of the evaporation/condensation coefficient β were used (see supplementary material). First, the averaged condensation coefficient β_g, which is close to the evaporation coefficient for the systems in equilibrium or quasi-equilibrium state, can be estimated in terms of thermodynamic potentials[34,51]

$$\frac{1-\langle\beta_g\rangle}{\langle\beta_g\rangle} = \exp\left(\frac{\langle\Delta G_{v\to l}\rangle}{RT}\right), \quad (1)$$

where $\Delta G_{v\to l} = G_l - G_v$ is the difference between the Gibbs free energies of molecules in a liquid and a vacuum, and averaging is carried out following Eqs. (S1) and (S2).[58] The values of $\langle\beta_g(T)\rangle$ can be corrected using averaged (over a set of conformers) function α_g obtained from the following equation:

$$\frac{1-\langle\alpha_g\rangle}{\langle\alpha_g\rangle} = \exp\left(\frac{\langle\Delta G_{l\to v}\rangle}{RT}\right), \quad (2)$$

where $\Delta G_{l\to v}$ is the change in the Gibbs free energy upon transfer of a molecule from liquid state into a vacuum to form the gas phase. The value of $\langle\alpha_g\rangle$ should be subtracted from $\langle\beta_g\rangle$ to consider the transfer between gas (instead of vacuum) and

liquid phases in equilibrium (or quasi-equilibrium) state

$$\langle \beta_{\Delta}(T) \rangle = \langle \beta_{g}(T) \rangle - \langle \alpha_{g}(T) \rangle. \quad (3)$$

Note that $\Delta G_{l \to v} > 0$, while $\Delta G_{v \to l} < 0$.

Alternative approaches to estimating the values of β using the TST are based on the expressions[51]

$$\beta_{V,g} = [1 - (V_l/V_g)^{1/3}] \exp(-\Delta G_{ev}/RT), \quad (4)$$

$$\beta_{V} = [1 - (V_l/V_g)^{1/3}] \exp\{-0.5/[(V_g/V_l)^{1/3} - 1]\}, \quad (5)$$

where V_l and V_g are the specific volumes of the liquid and gas phases, respectively. Subscript V indicates that the expression for β explicitly depends on the specific volumes. The definitions of all constants and coefficients and more detailed description of equations are given in the supplementary material. Averaged (over a set of conformers) values of β ($\langle \beta \rangle$) are also used later in the paper (see supplementary material[58]).

The CDM effects, which can contribute to the Gibbs free energies of evaporation, $\Delta G_{ev}(T)$, and solvation, $\Delta G_{s}(T)$, were analysed using the MSTor program[62,63] applied to *n*-dodecane at 300-1200 K. Ninety five stable conformers (see Tables S1-S3[58]) were selected based on the changes in the Gibbs free energy from 1000 conformers generated by ConfGen[62] and analysed using MSTor.[62,63] Note that the numbers referring to conformers under consideration (see Table S1[58]) are random and do not depend on the value of G (see Tables S2 and S3[58]). This was done to obtain a relatively random set of conformers at various $N \leq 95$ characterised by wide distributions of the values of G. The details of calculations are given in supplementary material.[58]

III. RESULTS AND DISCUSSION

There are several sets of factors, which are expected to affect the evaporation/condensation processes of *n*-dodecane droplets. First, these are those linked to structure, population, and transformation of various conformers of *n*-dodecane in the gas and liquid phases. Second, these are those due to features of the surroundings of the molecules at the surface and in the bulk of droplets and those related to orientation of evaporating/condensing molecules and a number of neighbouring molecules at the droplet surface. Third, these are temperature, total and partial gas pressures, and liquid and gas densities. Most of these factors will be analysed below using the QC approaches enhanced by empirical or model corrections.

The orientation of relatively long *n*-dodecane molecules (e.g., unbent conformer S1 is approximately 1.6 nm long) at the surfaces of droplets can affect the values of β. This orientation affects a number of neighbours of an evaporating molecule,[40,41] and, therefore, the energy which needs to be spent to remove the molecule into the gas phase (or into the interfacial layer) from the droplet surface. During condensation of *n*-dodecane molecules, the orientation of attacking molecules relative to the droplet surface and molecules at this surface (see Fig. 1(a) and Fig. S1[58]) can affect the accommodation coefficient.[40,41]

The analysis of these effects within the scope of the TST was based on consideration of corrected surface Gibbs free energy of solvation $w\Delta G_s$ at $w < 1$ instead of ΔG_s (as a measure of ΔG_{ev}) calculated for molecules in the bulk liquid. The correction factor w in $\Delta G_{ev} = \Delta G_{l \to g} = -w\Delta G_s$ was used.[41] Parameter $w < 1$ takes into account that the number of neighbours of an evaporating molecule at a surface is smaller than in the bulk liquid. Using 3D models of droplets,[40,41] one can assume that the value of w can be smaller for bent conformers and is expected to be in the range of 0.25–1. This effect was analysed for several conformers located perpendicular ($w = 1$, the evaporating molecule is located completely inside the droplet) or parallel ($w \approx 5/8$, the evaporating molecule is semi-submerged in the surface layer of the droplet) to the surface of the droplet (Fig. 2).

The MD FF approach can be used for modelling thermal swelling and evaporation of an *n*-dodecane nanodroplet (see Fig. 1(a) and Fig. S1[58]). The results based on this approach, as well as previous QC calculations,[40,41] indicate the presence of

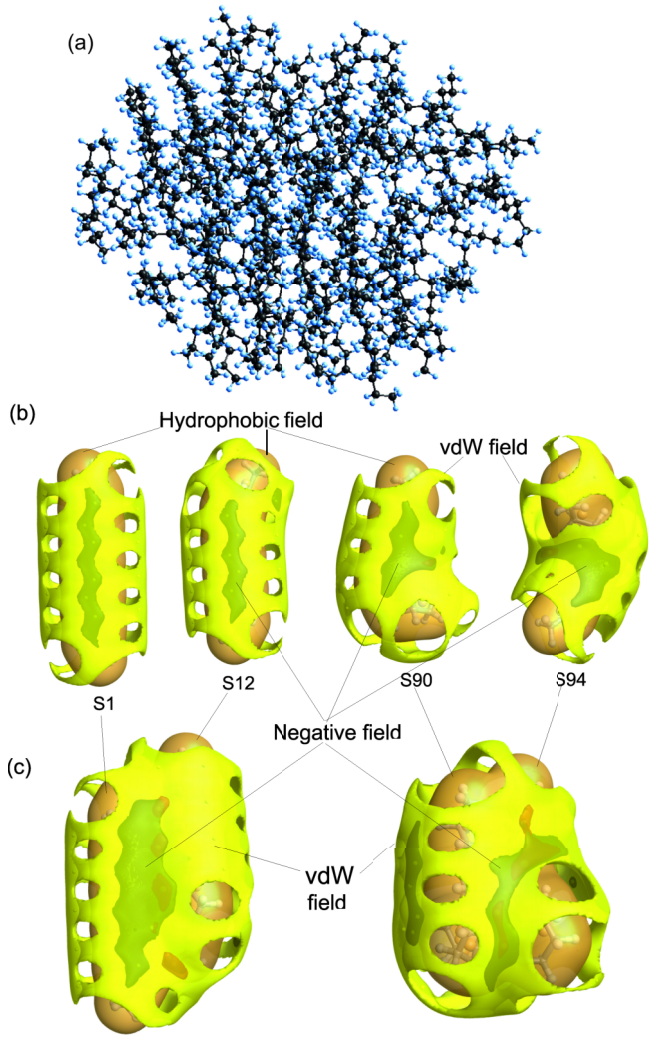

FIG. 1. (a) A nanodroplet (cluster) with 64 *n*-dodecane molecules used in the MD modelling of heating at 293 K for 20 ps and then at 400 K for 20 ps using MM + FF (VEGA ZZ[64] with NAMD[65]); ((b) and (c)) visualisation of the vdW, hydrophobic (describing regions with high hydrophobicity), and negative (due to positive charges on the H atoms) fields around the molecules (calculated using TorchLite[59,60]) for (b) individual conformers (S1, S12, S90, and S94) and for (c) conformers merged in dimers S1 and S12 and S90 and S94.

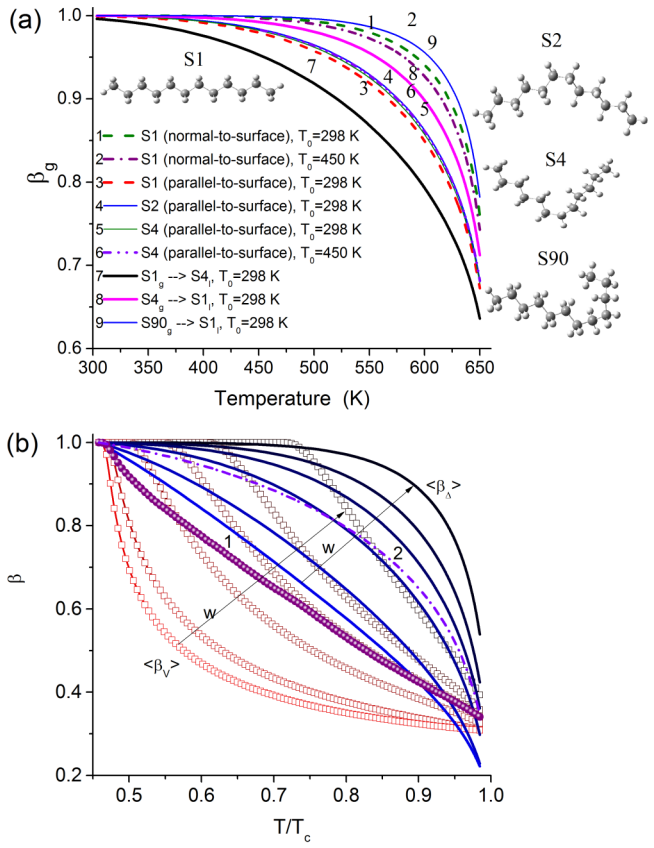

FIG. 2. Condensation coefficient *vs*. temperature. (a) β_g with two orientations of a molecule at the surface of a liquid *n*-dodecane droplet normal to the surface (w = 1) or parallel to the surface (w = 5/8)[40,41] for conformers S1, S2, S4, and S90. T_0 is the temperature for both phases in QC calculations. (b) Averaged $\langle\beta_\Delta\rangle$ (symbols) and $\langle\beta_V\rangle$ (curves) with CDM at w = 0.25, 0.3333, 0.5, 0.625, 0.75, and 1 (arrows correspond to increased values of w) and curves calculated based on arithmetic averaging (curves 1 and 2). Calculations were carried out using ωB97X-D/cc-pVTZ and SMD/ωB97X-D/cc-pVTZ for (a) selected conformers and (b) a collection of selected 73 conformers (see Table S2[58]) at pressure of 0.35 MPa.

various orientations of the molecules at the surface, as well as in the gas phase. Also, the molecules in both phases represent an ensemble of various conformers (see Fig. 1(b) and Table S1[58]). Strongly bent molecules (e.g., conformers S90 and S94 (Fig. 1)) are characterised by vdW and negative fields, different (especially around chain inflection) from those around linear (S1) or slightly bent (S12) ones (Figs. 1(b) and 1(c)). The former are characterised by higher values of the Gibbs free energy G (see Tables S2 and S3) than the latter. Small patches of negative fields (Figs. 1(b) and 1(c)) are attributed to positive charges on the H atoms (small negative charges are on the C atoms). These charges on the H atoms around the bent fragment increase from 0.08-0.09 a.u. in S1 to 0.11-0.12 a.u. in S90 or S94. Note that solvation in the *n*-dodecane medium results in a small increase in the atom charges in *n*-dodecane conformers. The changes in the fields around strongly bent conformers (Figs. 1(b) and 1(c)) can affect intermolecular interactions (Fig. 1(c)), and, therefore, the evaporation/condensation processes for various conformers.

At w = 1 (i.e., an evaporating molecule is completely imbedded into the droplet), the process is characterised by greater values of β_g (and smaller values of γ) in comparison with a molecule drifting parallel to the surface (Fig. 2(a)). The values of $\langle\beta_V\rangle$ and $\langle\beta_\Delta\rangle$ decrease (by two times or more at T/T_c = 0.6-0.8) with decreasing values of w from 1 to 1/2–1/4 (Fig. 2(b)). However, at higher temperatures ($T/T_c > 0.85$), this effect is less visible. In our calculations, w = 5/8 is used as an average value for surface molecules, since the curves averaged by w (Fig. 2(b), curves 1 and 2) are located close to the corresponding curves calculated at w = 5/8. Thus, molecules with bent chains and upright portions above the droplet surface plane can be more easily evaporated due to smaller contact area with neighbouring molecules, despite slightly increased polarisation of the bent chain (Fig. 1). This is one of the reasons for enhancement of the evaporation rate and reduction of the values of β due to the CDM effects. It should be noted that a sample ensemble with 73 conformers (used in the calculations with cc-pVTZ, Fig. 2(b)) is sufficiently wide to study the CDM effects (*vide infra*).

Molecules located in the interfacial layer outside the liquid droplet (see Figs. S1(b)-S1(e) in supplementary material[58]) undergo weak intermolecular interactions with molecules at the droplet surface. The difference in the Gibbs free energies of molecules in the gas phase and the interfacial layer is much smaller than that for the molecules in the gas and liquid phases. Therefore, it is not easy to estimate the values of β for transfer of the molecules between the interfacial layer and the gas phase in terms of the changes in the Gibbs free energy (the value of w should be very small, <0.1, for the interfacial layer). This could be done within the QC MD modelling,[40,41] and is not studied in our paper.

Note that the formation of vapour bubbles inside bulk liquid at $T \geq T_b \approx 489.5$ K (boiling point of *n*-dodecane) can enhance the evaporation process. The value of w for molecules evaporated into the bubbles can be greater than that for the molecules evaporated from the outer surface of droplets due to different signs of the surface curvature in these two cases. Therefore, the evaporation from the outer surface of droplets is faster than that into the bubbles. The bubble formation and the contribution of the interfacial layer are not studied in our paper.

Also, the values of β depend on the CDM in both phases and the details of the process of transfer between these phases. If the evaporation occurs without changes in the conformer structure, the orientation effects at the surface are predominant (Fig. 2(a)).[40,41] If CDM occurs during the transfer process, the value of β_g is lower for condensed conformers having higher Gibbs free energy in the gas phase than in the liquid phase. For example, the value of β_g is lower for $S1_g \rightarrow S4_l$ transfer (see Fig. 2(a), curve 7) than that for $S4_g \rightarrow S1_l$ transfer (see Fig. 2(a), curve 8) as S1 is a more stable conformer than S4 in both phases (see Tables S2 and S3[58]). The values of T_0 (298.15 or 450.0 K) for both phases in QC calculations of the Gibbs free energy weakly affect the values of β_g calculated with corrections described by Eq. (S4)[58] (see Fig. 2(a), curves 1 and 2 or 5 and 6). Therefore, the main part of the QC calculations was performed at T_0 = 298.15 K with the temperature corrections based on Eq. (S4).[58]

The density distribution functions of the changes in the Gibbs free energy during transfer of conformers between the gas and liquid phases or for CDM in the same phase (Fig. 3)

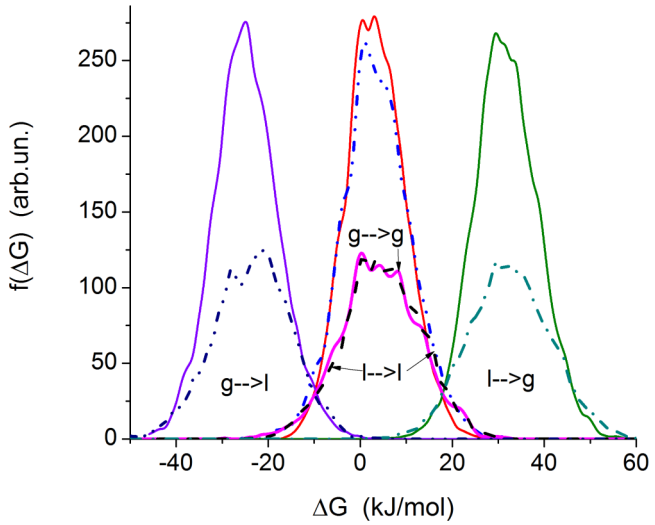

FIG. 3. The Gibbs free energy distribution functions, $f(\Delta G)$ for conformerisation during the transfer between phases $\Delta G_{g\to l}$ and $\Delta G_{l\to g}$ or in the same phase ($\Delta G_{g\to g}$ (solid curves) and $\Delta G_{l\to l}$ (dashed and dotted-dashed curves) (2)) are calculated from Eq. (6) at σ = 0.5 kJ/mol for 73 conformers (see Table S2[58]) with the cc-pVTZ basis set (lower curves) and 95 conformers with the cc-pVDZ basis set (upper curves).

can be calculated using the following equation:[66]

$$f(\Delta G) = (2\pi\sigma^2)^{-0.5} \sum_{i=1}^{N} \exp[-(\Delta G_i - \Delta G)^2/2\sigma^2], \quad (6)$$

where σ is the distribution variance.

This function for a smaller ensemble (73 conformers, calculated using cc-pVTZ) has a shape similar to that for a larger ensemble of 95 conformers (cc-pVDZ) (see Fig. 3). However, the latter is characterised by higher peaks due to the larger number of samples in the ensemble. Therefore, the calculations with the larger basis set (cc-pVTZ) were carried out for a smaller ensemble of the conformers than which was used in the calculations with the cc-pVDZ basis set.

As mentioned above, pressure in the gas phase affects the value of β. According to QC calculations, using Eqs. (S7) and (S11)[58] and CDM, the average values $\langle\beta_V\rangle$ increase with increasing pressure (see Fig. 4(a)). The effects of temperature on $\langle\beta_V\rangle$ at a constant pressure (volume of the gas phase increases with T) and at $p \sim T$ (due to restricted volume of the gas phase) are small. These effects are of the same order of magnitude as those due to CDM.

The effects of the basis sets used (cc-pVTZ or cc-pVDZ) and the number of conformers in the ensembles (73 or 95 conformers) on the values of β are small (Figs. 4(b) and S2). Therefore, calculations of β for all 95 conformers were carried out only with the smaller cc-pVDZ basis set, and the larger cc-pVTZ basis set was used for a smaller number of conformers but this set included the conformers with both minimal and maximal values of G in both phases (see Tables S2 and S3[58]).

The difference between the values of $\langle\beta_V\rangle$ and $\langle\beta_\Delta\rangle$ can be larger (Fig. 4(b)) than the one which can be attributed to ignoring changes in the n-dodecane density in the gas phase (affecting ΔG) in calculations of the values of $\langle\beta_\Delta\rangle$. In contrast to the calculations of $\langle\beta_\Delta\rangle$, the values of $\langle\beta_V\rangle$ were computed taking into account changes in the density in both phases with temperature which strongly affected the exponential part in Eq. (S8).[58] The application of Eq. (S7)[58] with the exponential part ignoring changes in the density of n-dodecane in the gas phase gives values of $\langle\beta_{V,g}\rangle$ close to $\langle\beta_g\rangle$ (Fig. 4(c)). Thus, ignoring the temperature dependence of the n-dodecane density in the gas phase on calculation of the values of $\langle\beta_\Delta\rangle$ with CDM, as well as fixing gas pressure used in calculations of the values of $\langle\beta_V\rangle$ with CDM, can lead to overestimation of the values

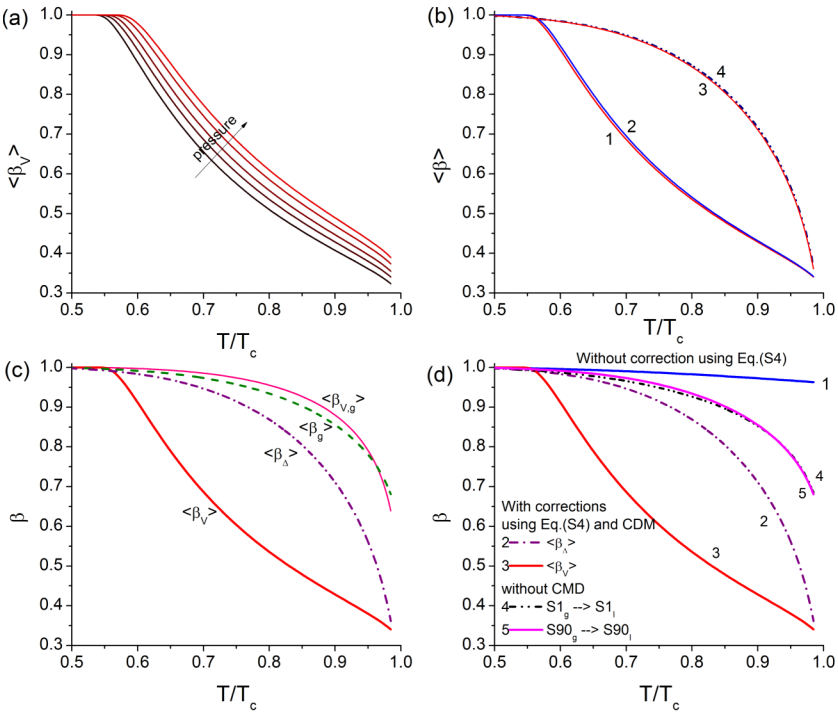

FIG. 4. (a) Effects of pressure (0.1, 0.35, 1, 3.5, and 10 MPa) in the gas phase on the average values of the evaporation/condensation coefficient ($\langle\beta_V\rangle$); (b) $\langle\beta_V\rangle$ (lower curves) and $\langle\beta_\Delta\rangle$ (upper curves) for 73 (curves 1 and 3) and 95 (curves 2 and 4) conformers calculated using cc-pVTZ and cc-pVDZ, respectively; (c) $\langle\beta_V\rangle$, $\langle\beta_{V,g}\rangle$, $\langle\beta_\Delta\rangle$, and $\langle\beta_g\rangle$; and (d) $\langle\beta_g\rangle$ (curve 1) without correction using Eq. (S4),[58] $\langle\beta_\Delta\rangle$ (curve 2) with corrections taking into account the dependence of the vaporisation enthalpy of n-dodecane on temperature and orientation of molecules at a surface of liquid n-dodecane ($\Delta G_{g\to l}$ = 5/8 ΔG_s at 298.15 K), $\langle\beta_V\rangle$ (curve 3), curves 4 and 5 refer to corrected β_Δ, but without CDM, for transfers of conformers S1 and S90, respectively. Selected 73 conformers in Figures (a)-(d) (see Table S2[58]) calculated with cc-pVTZ by ωB97X-D and SMD/ωB97X-D and 95 conformers in Figure (b) (see Table S3[58]) were calculated with the cc-pVDZ basis set at (a) various pressures or (b)-(d) 0.35 MPa.

of $\langle\beta_\Delta\rangle$ and underestimation of the values of $\langle\beta_V\rangle$ since, in the restricted volume, pressure increases with temperature (see Eq. (S9)[58]). This leads to the corresponding increase in $\langle\beta_V\rangle$ (Fig. 4(a)).

Analysing the influences of temperature, pressure, and gas/liquid density on β, one can anticipate that the application of Eq. (S4)[58] can give better results than direct calculations of the Gibbs free energy of evaporation $\Delta G_{ev}(T) = -\Delta G_s(T)$ based on the SMD method to calculate $\Delta G_s(T)$ at $0.45 < T/T_c < 1.0$.[40,41] The reasons for overestimation of $-\Delta G_s(T)$ in direct SMD calculations at $T > 300$ K can be linked to underestimation of a decrease in the liquid density with temperature. This can affect some physical characteristics, including permittivity and polarisability, and cause reduction of short-range intermolecular vdW and other interactions. The latter are related to increased average distances between molecules. This leads to overestimation of the values of β (Fig. 4(d), curve 1) in comparison with the corrected values of $\langle\beta_\Delta\rangle$ (Fig. 4(d), curve 2), and this difference increases with temperature.

The effect of CDM on the evaporation/condensation processes can be seen from the comparison of $\langle\beta_\Delta\rangle$ with CDM correction (Fig. 4(d), curve 2) and β_Δ without CDM correction (see Fig. 4(d), curves 4 and 5). Close results (Fig. 4(d), curves 4 and 5) observed for $S1_g \rightarrow S1_l$ (S1 with the ideal linear structure has low Gibbs free energy) and $S90_g \rightarrow S90_l$ (S90 with a strongly bent structure, see Fig. 1(b) and Table S1,[58] has high Gibbs free energy, see Tables S2 and S3[58]) can be explained by similar solvation effects for these conformers. This closeness leads to closeness in the changes in the Gibbs free energy during evaporation/condensation and solvation processes (Fig. 3). Thus, the evaporation/condensation process is expected to be affected by the transformation of conformers. This effect can be related to the fact that the difference in the Gibbs free energy for various conformers in the gas and liquid phases can be smaller than that for the same conformers in these two phases. As follows from our analysis, $\langle\beta_V\rangle < \langle\beta_\Delta\rangle$ in a wide temperature range (see Fig. 4(d), curves 2 and 3). Note that the changes in the gas phase density *vs.* T and p were taken into account in calculations of $\langle\beta_V\rangle$ but not those of $\langle\beta_\Delta\rangle$.

MD simulations with various potentials and approaches used to compute β[14,35] give smaller values than $\langle\beta_g\rangle$ and $\langle\beta_\Delta\rangle$ obtained using QC taking into account the CDM, especially at $T/T_c > 0.7$ (Fig. 5). This can be related to the underestimation of intermolecular interactions in the liquid *n*-dodecane, described by the MD FF, and in the gas phase, described by QC, at high temperatures (Fig. 5). The values of $\langle\beta_V\rangle$, computed using QC (TST), taking into account the CDM and changes in the gas phase density, are closer to $\langle\beta_\Delta\rangle$ than those computed using the MD FF for structureless LJ fluids and those computed based on a simplified model of an *n*-dodecane molecule (including united atom model). The values of $\langle\beta_V\rangle$ are slightly larger than the latter only at $T/T_c > 0.75$ due to underestimation of intermolecular interactions in the gas phase at high temperatures by MD FF.

$\Delta G_{l\rightarrow g}$ (estimated at $T_0 = 298.15$ K in Eq. (S4)[58]), corresponding to the process $S90_l \rightarrow S1_g$ (see Tables S2 and S3[58]), makes a relatively small contribution to the evaporation of *n*-dodecane since conformer S90 has ΔG_s higher than that of S1

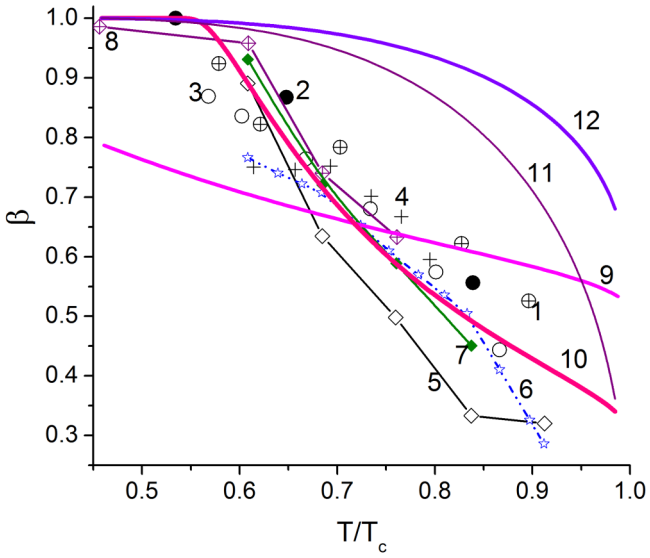

FIG. 5. Comparison of the values of the evaporation coefficient, predicted by MD FF (symbols 1-4, curves 5-8) and QC (curves 9-12) models. Symbols (1-4) refer to the models for structureless LJ fluids with various input parameters,[52] curves 5 and 7 refer to the results obtained based on the united atom model reported in Ref. 13 and in Ref. 14, respectively, curve 6 refers to the results of calculations based on the TST model reproduced from Ref. 13, curve 8 is based on the results of calculations using the model described by Mizuguchi *et al.*[35] The following QC processes were considered: $S90_l \rightarrow S1_g$ (curve 9) with $\Delta G_{l\rightarrow g} = 3.3$ kJ/mol at $T_0 = 298.15$ K. Also the curves calculated based on the averaging of the contributions of 73 conformers (see Table S2[58]) for $\langle\beta_V\rangle$ (curve 10), $\langle\beta_\Delta\rangle$ (curve 11), and $\langle\beta_g\rangle$ (curve 12) at 0.35 MPa and $w = 5/8$ are presented. QC calculations were performed using ωB97X-D/cc-pVTZ and SMD/ωB97X-D/cc-pVTZ.

by 23.7 kJ/mol. Therefore, the population of S90 conformers in liquid and gaseous *n*-dodecane is expected to be small. The same conclusion applies to other conformers with high Gibbs free energy (Fig. 3). The values of $\langle\Delta G_{l\rightarrow g}\rangle$ for all possible transfers for all conformers under consideration are greater than those for $S90_l \rightarrow S1_g$. The values of $\langle\beta_g\rangle$ and $\langle\beta_\Delta\rangle$ at $T/T_c > 0.65$ are greater than $\langle\beta_V\rangle$ or those calculated using the MD FF methods (Fig. 5(a)).[6,8,14]

The CDM effect on β decreases with increasing temperature (Fig. 5). The CDM effects on the changes in the values of β are similar to those due to pressure (Fig. 4(a)). However, at temperatures close to T_c, the pressure effects are stronger than those of the CDM.

A decrease in the intermolecular vdW interaction energy with temperature due to reduction of the liquid density results in a decrease in the values of β. The increase in the vdW interaction energy (related to the size of evaporated molecules or increase in the number of neighbours, see Fig. 2(b)) leads to a decrease in the values of γ.[40,41] Similar results were obtained for evaporating dimers[41] and trimers of molecules. The CDM effects leading to decreasing in β (see Figs. 4 and 5) cause increasing in the evaporation rate (Fig. 6, curve 2) and decreasing in the evaporation time (Fig. 6, curve 4) in comparison with those computed without consideration of the CDM effects (see Fig. 6, curves 1 and 3). These effects are attributed to reduction in the interactions of the evaporating molecules with neighbours and favourable changes in the Gibbs free energy of evaporation of certain conformers during their transfer into the gas phase.

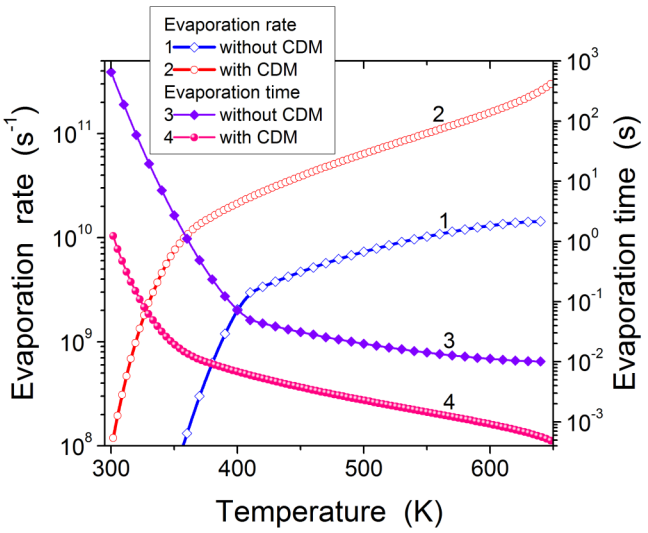

FIG. 6. Comparison of the evaporation rate γ (curves 1 and 2) and evaporation time (curves 3 and 4) of an n-dodecane microdroplet (droplet radius 2.65 μm with number of molecules 1.46×10^8 and pressure 3.5 MPa) not taking CDM into account (curves 1 and 3) and taking CDM into account (curves 2 and 4). Seventy-three conformers (see Table S2[58]) calculated using ωB97X-D/cc-pVTZ and SMD/ωB97X-D/cc-pVTZ were studied.

IV. CONCLUSION

The conformation-dependent evaporation/condensation processes of n-dodecane have been studied using quantum chemical DFT (functional ωB97X-D with the cc-pVTZ and cc-pVDZ basis sets) and SMD methods. Zero-point and thermal corrections to the Gibbs free energy in the gas phase and additional solvation terms for the molecules in the liquid phase have been taken into account. The geometry of 95 conformers has been optimised using ωB97X-D/cc-pVTZ. The TST has been applied to estimate the values of the evaporation/condensation coefficient. It is shown that the effects of conformerisation/cross-conformerisation and changes in the surroundings (number of adjacent molecules at a droplet surface) of evaporating molecules, as well as temperature, pressure, and gas and liquid density, play important roles in the evaporation/condensation processes of n-dodecane. The range of changes in the Gibbs free energy of small ensembles of selected conformers is shown to be more important than the numbers of conformers in the ensembles. This allows us to focus our analysis on only two conformers with maximal and minimal values of G in both phases. The predicted values of β *vs*. temperature are expected to be close to those inferred from the analysis of all 95 conformers. Changes in the interactions of evaporating molecules with the surroundings in the surface layer of a droplet are shown to affect β more strongly than the conformerisation and cross-conformerisation of the molecules in the gas and liquid phases or pressure in the gas phase. Also, the CDM effects are shown to be maximal at $T/T_c = 0.6$-0.7 and decrease with decreasing or increasing temperatures. They become negligible at $T/T_c < 0.55$ or T/T_c close to 1.

To enhance the reliability of the approach developed in our study, corrections to be applied in the analysis of the changes in the Gibbs free energy of evaporating/condensing molecules are suggested. These corrections are based on (i) the tabulated (experimental) data for the temperature dependence of the evaporation enthalpy and the density of the gas and liquid phases of n-dodecane and (ii) the differences in the surroundings of molecules at a droplet surface and in bulk liquid. The approach developed in our paper gives values of β which are close to β calculated for structureless LJ fluids and to β calculated for n-dodecane using MD FF methods, except at temperatures close to the critical temperatures.

ACKNOWLEDGMENTS

The authors are grateful to the EPSRC (UK) (Grant No. EP/J006793/1) for the financial support of this project. The use of NSCCS (http://www.nsccs.ac.uk/) and HECToR/ARCHER (http://www.archer.ac.uk/) supercomputers with a set of quantum chemical programs is gratefully acknowledged.

[1]M. A. Silberberg, *Chemistry—The Molecular Nature of Matter and Change*, 4th ed. (McGraw-Hill, New York, 2006).
[2]*Handbook of Atomization and Sprays*, edited by V. Ashgriz (Springer, Heidelberg, 2011).
[3]S. Fujikawa, T. Yano, and M. Watanabe, *Vapor-Liquid Interfaces, Bubbles and Droplets* (Springer, Heidelberg, 2011).
[4]M. B. Mcelroy, *The Atmospheric Environment* (Princeton University Press, Princeton, 2002).
[5]*Evaporation Condensation and Heat Transfer*, edited by A. Ahsan (InTech, Rijeka, Croatia, 2010).
[6]S. S. Sazhin, *Droplets and Sprays* (Springer, London, 2014).
[7]S. Chapman and T. G. Cowling, *The Mathematical Theory of Nonuniform Gases* (Cambridge University Press, Cambridge, 1970).
[8]S. S. Sazhin, Prog. Energy Combust. Sci. **32**, 162 (2006).
[9]J. Tamim and W. L. H. Hallett, Chem. Eng. Sci. **50**, 2933 (1995).
[10]A. M. Lippert and R. D. Reitz, SAE Tech. Pap. **1997**, 972882.
[11]W. L. H. Hallett, Combust. Flame **121**, 334 (2000).
[12]G.-S. Zhu and R. D. Reitz, Int. J. Heat Mass Transfer **45**, 495 (2002).
[13]B.-Y. Cao, J.-F. Xie, and S. S. Sazhin, J. Chem. Phys. **134**, 164309 (2011).
[14]J.-F. Xie, S. S. Sazhin, and B.-Y. Cao, Phys. Fluids **23**, 112104 (2011).
[15]S. S. Sazhin, M. Al Qubeissi, R. Nasiri, V. M. Gun'ko, A. E. Elwardany, F. Lemoine, F. Grisch, and M. R. Heikal, Fuel **129**, 238 (2014).
[16]H. Yanagihara, I. Stanković, F. Blomgren, A. Rosén, and I. Sakata, Combust. Flame **161**, 541 (2014).
[17]S. Cheng, J. B. Lechman, S. J. Plimpton, and G. S. Grest, J. Chem. Phys. **134**, 224704 (2011).
[18]M. S. Hanchak, M. D. Vangsness, L. W. Byrd, and J. S. Ervin, Int. J. Heat Mass Transfer **75**, 196 (2014).
[19]M. Knott, H. Vehkamäki, and I. J. Ford, J. Chem. Phys. **112**, 5393 (2000).
[20]H. W. Hu and G. H. Tang, Appl. Therm. Eng. **62**, 671 (2014).
[21]S.-M. Kim and I. Mudawar, Int. J. Heat Mass Transfer **77**, 627 (2014).
[22]A. Lotfi, J. Vrabec, and J. Fischer, Int. J. Heat Mass Transfer **73**, 303 (2014).
[23]I. J. Ford and S. A. Harris, J. Chem. Phys. **120**, 4428 (2004).
[24]P. Sosnowski, A. Petronio, and V. Armenio, Int. J. Heat Mass Transfer **66**, 382 (2013).
[25]L. Yang, X. Quan, P. Cheng, and Z. Cheng, Int. J. Heat Mass Transfer **78**, 460 (2014).
[26]M. E. V. da Silva, K. Schwarzer, B. Hoffschmidt, F. P. Rodrigues, T. Schwarzer, and P. A. C. Rocha, Renewable Energy **53**, 174 (2013).
[27]S. Natarajan, S. A. Harris, and I. J. Ford, J. Chem. Phys. **124**, 044318 (2006).
[28]X. Lv and B. Bai, Appl. Therm. Eng. **65**, 24 (2014).
[29]B. Peng, W. He, X. Hao, Y. Chen, and Y. Liu, Comput. Mater. Sci. **87**, 260 (2014).
[30]S. Takata and F. Golse, Eur. J. Mech. - B/Fluids **26**, 105 (2007).
[31]M. Bond and H. Struchtrup, Phys. Rev. E **70**, 061605 (2004).
[32]V. K. Badam, V. Kumar, F. Durst, and K. Danov, Exp. Therm. Fluid Sci. **32**, 276 (2007).
[33]W. S. Drisdell, C. D. Cappa, J. D. Smith, R. J. Saykally, and R. C. Cohen, Atmos. Chem. Phys. **8**, 6699 (2008).
[34]M. Zientara, D. Jakubczyk, K. Kolwas, and M. Kolwas, J. Phys. Chem. A **112**, 5152 (2008).

[35]H. Mizuguchi, G. Nagayama, and T. Tsuruta, *Seventh International Conference on Flow Dynamics* (Tohoku University Press, Sendai, Japan, 2010), p. 386.
[36]J.-F. Xie, S. S. Sazhin, I. N. Shishkova, and B.-Y. Cao, in *Proceedings of CHT12-MP02 International Symposium on Advances in Computational Heat Transfer*, *1–6 July 2012* (Begell House, Inc., Bath, UK, 2012).
[37]J.-F. Xie, S. S. Sazhin, and B.-Y. Cao, J. Therm. Sci. Technol. **7**, 288 (2012).
[38]I. K. Ortega, O. Kupiainen, T. Kurtén, T. Olenius, O. Wilkman, M. J. Mcgrath, V. Loukonen, and H. Vehkamäki, Atmos. Chem. Phys. **12**, 225 (2012).
[39]O. Kupiainen, I. K. Ortega, T. Kurtén, and H. Vehkamäki, Atmos. Chem. Phys. **12**, 3591 (2012).
[40]V. M. Gun'ko, R. Nasiri, S. S. Sazhin, F. Lemoine, and F. Grisch, Fluid Phase Equilib. **356**, 146 (2013).
[41]V. M. Gun'ko, R. Nasiri, and S. S. Sazhin, Fluid Phase Equilib. **366**, 99 (2014).
[42]C. A. Hunter, Chem. Sci. **4**, 834 (2013).
[43]*Encyclopedia of Computational Chemistry*, edited by P. v. R. Schleyer (John Wiley & Sons, New York, 1998).
[44]P. W. Atkins and R. Friedman, *Molecular Quantum Mechanics*, 4th ed. (Oxford University Press, Oxford, 2005).
[45]COSMOthermX, version C30_1301 December 12th COSMOlogic GmbH & Co., KG, Leverkusen, Germany 2012.
[46]Y. Fujitani, K. Saitoh, A. Fushimi, K. Takahashi, S. Hasegawa, K. Tanabe, S. Kobayashi, A. Furuyama, S. Hirano, and A. Takami, Atmos. Environ. **59**, 389 (2012).
[47]S. Dirbude, V. Eswaran, and A. Kushari, Atomization Sprays **21**, 787 (2011).
[48]G. Guéna, C. Poulard, and A. M. Cazabat, Colloids Surf., A **298**, 2 (2007).
[49]M. Heldmann, T. Knorsch, and M. Wensing, SAE Int. J. Engines **6**, 1213 (2013).
[50]L. Zigan, I. Schmitz, A. Flügel, M. Wensing, and A. Leipertz, Fuel **90**, 348 (2011).
[51]G. Nagayama and T. Tsuruta, J. Chem. Phys. **118**, 1392 (2003).
[52]A. Lotfi, J. Vrabec, and J. Fischer, Int. J. Heat Mass Transfer **73**, 303 (2014).
[53]M. J. Frisch, G. W. Trucks, H. B. Schlegel, G. E. Scuseria, M. A. Robb, J. R. Cheeseman, G. Scalmani, V. Barone, B. Mennucci, G. A. Petersson, H. Nakatsuji, M. Caricato, X. Li, H. P. Hratchian, A. F. Izmaylov, J. Bloino, G. Zheng, J. L. Sonnenberg, M. Hada, M. Ehara, K. Toyota, R. Fukuda, J. Hasegawa, M. Ishida, T. Nakajima, Y. Honda, O. Kitao, H. Nakai, T. Vreven, J. A. Montgomery, Jr., J. E. Peralta, F. Ogliaro, M. Bearpark, J. J. Heyd, E. Brothers, K. N. Kudin, V. N. Staroverov, T. Keith, R. Kobayashi, J. Normand, K. Raghavachari, A. Rendell, J. C. Burant, S. S. Iyengar, J. Tomasi, M. Cossi, N. Rega, J. M. Millam, M. Klene, J. E. Knox, J. B. Cross, V. Bakken, C. Adamo, J. Jaramillo, R. Gomperts, R. E. Stratmann, O. Yazyev, A. J. Austin, R. Cammi, C. Pomelli, J. W. Ochterski, R. L. Martin, K. Morokuma, V. G. Zakrzewski, G. A. Voth, P. Salvador, J. J. Dannenberg, S. Dapprich, A. D. Daniels, O. Farkas, J. B. Foresman, J. V. Ortiz, J. Cioslowski, and D. J. Fox, Gaussian 09, Revision D.01, Gaussian, Inc., Wallingford CT, 2013.
[54]J.-D. Chai and M. Head-Gordon, Phys. Chem. Chem. Phys. **10**, 6615 (2008).
[55]K. Yang, J. Zheng, Y. Zhao, and D. G. Truhlar, J. Chem. Phys. **132**, 164117 (2010).
[56]A. V. Marenich, C. J. Cramer, and D. G. Truhlar, J. Phys. Chem. B **113**, 6378 (2009).
[57]A. D. Becke, J. Chem. Phys. **140**, 18A301 (2014).
[58]See supplementary material at http://dx.doi.org/10.1063/1.4905496 for describing calculation models, some calculation results, and structures of 95 conformers of n-dodecane.
[59]T. Cheeseright, M. Mackey, S. Rose, and J. G. Vinter, Expert Opin. Drug Discovery **2**, 131 (2007).
[60]T. Cheeseright, M. Mackey, S. Rose, and J. G. Vinter, J. Chem. Inf. Model. **46**, 665 (2006).
[61]G. A. Zhurko and D. A. Zhurko, Chemcraft (version 1.7, build 382) (2014). http://www.chemcraftprog.com.
[62]J. Zheng, S. L. Mielke, K. L. Clarkson, and D. G. Truhlar, Comput. Phys. Commun. **183**, 1803 (2012).
[63]J. Zheng, R. Meana-Pañeda, and D. G. Truhlar, Comput. Phys. Commun. **184**, 2032 (2013).
[64]A. Pedretti, L. Villa, and G. Vistoli, J. Comput.-Aided Mol. Des. **18**, 167 (2004).
[65]J. C. Phillips, R. Braun, W. Wang, J. Gumbart, E. Tajkhorshid, E. Villa, C. Chipot, R. D. Skeel, L. Kale, and K. Schulten, J. Comput. Chem. **26**, 1781 (2005).
[66]V. M. Gun'ko and V. V. Turov, *Nuclear Magnetic Resonance Studies of Interfacial Phenomena* (CRC Press, Boca Raton, 2013).